X-ray absorption spectroscopy and imaging of heterogeneous hydrothermal mixtures using a diamond microreactor cell

John L. Fulton,[a] John G. Darab, and Markus M. Hoffmann
Fundamental Science Division, Pacific Northwest National Laboratory, Richland, Washington 99352

(Received 31 August 2000; accepted for publication 8 January 2001)

Hydrothermal synthesis is an important route to novel materials. Hydrothermal chemistry is also an important aspect of geochemistry and a variety of waste remediation technologies. There is a significant lack of information about the speciation of inorganic compounds under hydrothermal conditions. For these reasons we describe a high-temperature, high-pressure cell that allows one to acquire both x-ray absorption fine structure (XAFS) spectra and x-ray transmission and absorption images of heterogeneous hydrothermal mixtures. We demonstrate the utility of the method by measuring the Cu(I) speciation in a solution containing both solid and dissolved Cu phases at temperatures up to 325 °C. X-ray imaging of the various hydrothermal phases allows micro-XAFS to be collected from different phases within the heterogeneous mixture. The complete structural characterization of a soluble bichloro-cuprous species was determined. *In situ* XAFS measurements were used to define the oxidation state and the first-shell coordination structure. The Cu–Cl distance was determined to be 2.12 Å for the $CuCl_2^-$ species and the complete loss of tightly bound waters of hydration in the first shell was observed. The microreactor cell described here can be used to test thermodynamic models of solubility and redox chemistry of a variety of different hydrothermal mixtures. [DOI: 10.1063/1.1351836]

I. INTRODUCTION

One route to synthesis of novel materials is hydrothermal synthesis. For instance, formation of ultrafine particles having precisely controlled chemical structure can be obtained from flow-through hydrothermal reactors.[1,2] Another area of interest for hydrothermal chemistry pertains to conversion of aqueous, radioactive solutions and sludges derived from various Department of Energy (DOE) defense waste inventories into glass forms for long-term storage.[3,4] In the latter case it is important to understand the aqueous heterogeneous chemistry that underlies the pretreatment and early stages of the vitrification processes. Finally, the chemistry of transition metals such as Cu under hydrothermal conditions ($T > 100$ °C) is of interest to a diverse number of fields including materials synthesis, geochemistry,[5] and metal corrosion. Whereas thermodynamic models are widely employed to predict the oxidation states, coordination, and solid–liquid equlibria, these techniques are less reliable for temperatures just below and above the critical point of water ($T_c = 375$ °C). Thus it is of interest to conduct *in situ* studies that will provide a complete characterization of such hydrothermal species. Methods that probe the macroscopic properties of these solutions such as solubility, conductivity, or potentiometric measurements provide important information about speciation but often the interpretation of these types of data relies heavily on assumptions about oxidation state and coordination structure of the equilibria species. Electronic or vibrational spectroscopies also provide information that can be successfully applied to a limited number of systems that have optically active modes.[6–8]

Another challenge for studies of hydrothermal systems is that many systems of interest are heterogeneous, with one or more solid phases in equilibrium with a liquid and/or a vapor phase. Often, solid phases are intentionally present to control the equilibrium fugacity, *p*H, or oxidation potential. Further, highly concentrated solutions or slurries of interest for waste processing may consist of a complex solid matrix in equilibrium with a liquid phase. In this article we describe a method to acquire both an x-ray image of heterogeneous hydrothermal mixtures and x-ray absorption spectra that provide information on the oxidation states and coordination structure of the individual liquid and solid phases. We use this technique to explore the hydrothermal chemistry of two different Cu mixtures.

X-ray absorption fine structure (XAFS) studies of ions in water at high temperatures provide important insights into the exact nature of ion–water and ion–ion associations.[9–16] XAFS studies yield mostly the first-shell structure about ions and numerous studies have now demonstrated that this technique is suitable to temperatures well above 400 °C for these aqueous systems. It is this first-shell structure that is of utmost importance for controlling the thermodynamics of these systems. High-brilliance x-ray synchrotron sources allow *in situ* measurements of oxidation states (from the pre-edge region) and coordination structures (from the extended fine structure region). We report a method to collect *in situ* XAFS spectra on a Cu multiphase system, thus permitting the measurements of kinetics and equlibria for heterogeneous hydrothermal mixtures.

The diamond microreactor cell (DMRC) used in these systems utilizes a simple design in which the heterogeneous

[a]Corresponding author; electronic mail: jl_fulton@pnl.gov

mixture of interest is sealed between two diamond x-ray windows. The body of the cell is constructed from a material that is noninterfering with the chemistry of interest. For many hydrothermal systems of interest to the areas of geochemistry and typical industrial processes, the pressures are well below 1 kbar. Use of diamond anvil cells is not required for this pressure regime and the alternate design described here provides several advantages. Foremost are the larger apertures (~2 mm) and the longer available x-ray pathlengths (100 μm–10 cm). The larger aperture allows for much easier imaging and micro-XAFS acquisitions. The longer pathlengths are suitable for acquisition of high signal-to-noise x-ray transmission spectra under a wide range of concentrations. These features enable many different types of studies of the speciation and equlibria of heterogeneous samples under hydrothermal conditions. For homogeneous liquid or supercritical samples the previously described flow-cell technique is a preferred approach.[17,18] Several designs suitable for hydrothermal experiments have been reported.[9,11,13,19,20] Diamond anvil cells have also been used for hydrothermal x-ray experiments at high temperature and pressure.[21,22]

These x-ray techniques are demonstrated on Cu-containing systems in which significant redox and coordination chemistry occur under hydrothermal conditions. One of the systems for this study initially contains two different solid phases of copper (CuO and Cu^0) in a concentrated HCl/NaCl solution. At high temperatures, the reduction of the CuO occurs to form a soluble $CuCl_2^-$ species. The importance of this species for transport of copper in geochemical systems is well known.[23,24] We demonstrate how imaging and micro-XAFS allow complete characterization of the soluble hydrothermal species and the characterization of chemical changes in solid phases that are in equilibrium with the liquid phase. X-ray imaging with a highly focused beam is a prerequisite to acquisition of XAFS spectra of different homogeneous regions within the sample cell. The x-ray image allows one to ascertain the number of and the types of phases (solid, liquid, vapor) present in the mixture. Then using the same optical configuration one can subsequently acquire XAFS spectra of the different homogenous regions. In addition, XAFS images can be acquired at energies near the absorption edge by taking the ratio of two images at slightly different energies around prominent absorbance features. Such XAFS images can provide a map of the two-dimensional distribution of a particular element in the sample or the distribution of oxidation states of that element.

II. EXPERIMENT

The copper oxide (CuO) and copper chloride ($CuCl_2$) used had reported purities of 99.99% and were used as received from Alpha Aesar. Two different solutions were examined in this study and the starting concentrations under ambient conditions are reported in Table I. The hydrothermal chemistry of the solution ''A'' was examined at 100 °C, whereas that of solution ''B'' was examined 325 °C.

The cell was of a static or ''batch'' design in which solutions were prepared and loaded under ambient conditions and then sealed between the two x-ray windows. It is similar in design to previously described hydrothermal flow cells.[17,18] Figure 1 shows a photographic enlargement of the core of the diamond microreactor cell. The aqueous sample is contained between two 3 mm outer diameter (o.d.)×0.5 mm thick diamond windows and within a 3 mm o.d.×2 mm inner diameter (i.d.)×2 mm long metallic tube (copper in this case). The sample is loaded by removing the upper window and then adding the liquid and/or solid components to the interior region. The upper window is replaced and then the window-retaining nut is tightened to preload the disk springs. The disk springs maintain a constant sealing force against the diamond window and they oppose the force generated as the solution pressure increases at higher temperatures. The disk springs also compensate for small dimension changes that occur at high temperatures such as differential thermal expansion of the different materials of construction and for the plastic deformation of the internal sample tube. Disk springs (Schnorr Co.) constructed from a high temperature alloy (Nimonic 90) were used.

TABLE I. Starting formulations corresponding to the solutions in Figs. 2(A) and 2(B). Concentrations are expressed in molality.

Solution	Composition
A	CuO Cu^0 0.5 m NaCl 0.3 m HCl (*p*H of 0.5)
B	0.2 m $CuCl_2$ Cu^0 0.03 m HCl (*p*H of 1.5)

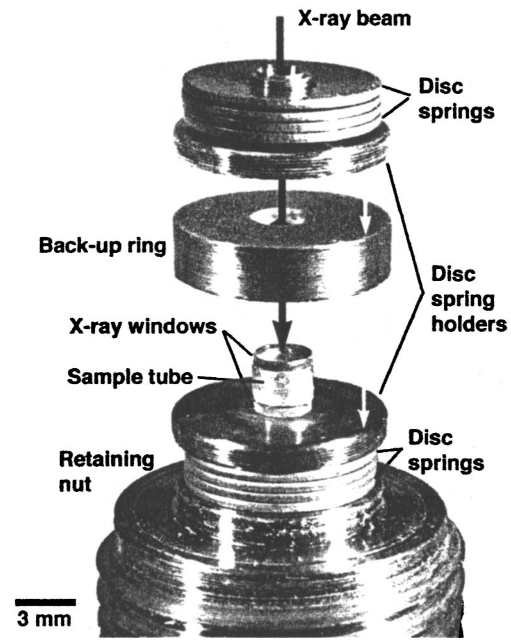

FIG. 1. Photograph of the partially disassembled diamond microreactor cell. The upper window-retaining nut and the cell body are not shown for clarity. The back-up ring, the upper assembly of the disk springs, and the holder are shown elevated.

The internal sample tube can be constructed from a wide variety of corrosion resistant materials such as Pt or Ti alloys. For the ultimate in corrosion resistant behavior, a diamond tube fabricated by laser cutting could be used for this sample ring either singly or stacked to provide the pathlength of interest. Alternately, pure metals like Cu or Fe could be used for specific chemical systems. In these cases a thin layer of the inner surface may be consumed as a part of the inorganic reaction. Such a strategy can avoid contamination from other cell metals when studying mixtures that are extremely corrosive. One requirement for any of these materials is that the seal-forming ends that contact the diamond surface must be optically flat and have a good polish. Another requirement when using lower strength materials such as Cu for the internal sample tube, is that there be a tight fit between the outer diameter of the sample tube and the inner diameter of the back-up ring. For use of a soft, low tensile-strength material such as copper, the tightly fitting back-up ring provides support under high pressure conditions. All remaining parts of the cell are constructed from a titanium alloy (Ti/6%Al/4%V) that provides good strength at high temperatures. The cell body is a larger cylinder having an o.d. of 3.5 cm and a length of 4 cm. The perimeter of this cylinder is drilled with several 3.2 mm holes in the axial direction to accept the platinum-resistive temperature probes and the small cylindrical resistance heaters.

The internal volume of the cell was about 6 μl, which is considerably larger than for a diamond anvil cell. The larger size allows for quantitative additions of solid and liquid components. In these studies the height of the sample tube was 2 mm (the x-ray pathlength). A range of different pathlengths from several hundreds of microns to 10 cm is available with the same design by simply changing the length of the sample tube and the back-up ring.

After loading the cell with the sample, the cell was clad in multiple layers of a fiber insulating material to minimize the radiative heat losses. The cell was then placed in a vacuum can to eliminate the convective heat losses. This method provides a high degree of temperature uniformity that is essential for acquisition of low-noise XAFS spectra. The temperature of the cell was maintained to within ± 1 °C using a three-mode controller (Omega, No. CN3000) with platinum resistive probes. The approximate Cu concentrations in the homogeneous, liquid microphase regions can be determined from the height of the copper absorption edge after calibration with appropriate standards.

The copper *K*-edge (8979 eV) XAFS spectra were collected on the insertion device beamline (ID-20, PNC-CAT) at the Advanced Photon Source (Argonne National Laboratory). A single, 15 min scan was sufficient to obtain high quality spectra at any position within the sample cell. For imaging studies, a 10 μm pinhole was placed in the unfocused beam. The sample cell was then rastered through a 3 $\times$3 mm sq area in order to obtain the 130$\times$130 element image. For acquisition of the Cu XAFS spectra, a 100 μm pinhole was substituted for the 10 μm pinhole.

For these studies, synthetic single-crystal diamond windows were used for the acquisition of the Cu (*K* edge 8979 eV) spectra. The windows contributed no significant artifacts to the acquired Cu XAFS spectra such as those that can result from diamond window Bragg reflections. However at energies above about 10 000 eV, single-crystal diamond has numerous Bragg reflections that interfere with the XAFS. There are many strategies that can be employed to successfully remove these artifacts. Since these reflections have a very narrow bandwidth, often one or two affected data points can be manually deleted from the data set. Alternatively, two or more different spectra can be acquired with slightly different cell rotations relative to the incident beam. This moves the spectral positions of the Bragg peaks so that a complete spectrum can be reconstructed. This simple procedure for removal of Bragg peaks is successful in many cases[25] although the special difficulties encountered in these types of procedures are well known.[26]

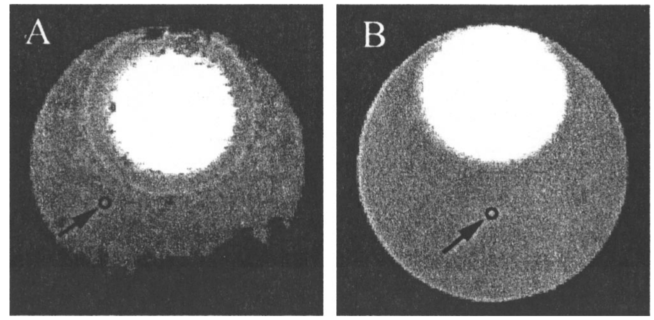

FIG. 2. X-ray transmission images through the diamond microreactor cell for solution A at 100 °C and for solution B at 325 °C. The composition of the copper solutions in A and B are reported in Table I. The large circle at the top of the cell is a vapor-phase bubble. In A, the granular material along the lower perimeter of the cell is CuO and/or Cu_2O solid. The small circles in both images indicate the size and location of the x-ray beam that was used to acquire the XAFS spectra reported in Fig. 3. The internal diameter of the cell is 2 mm.

Analysis of the XAFS data[27–29] was accomplished using a well established method that is reported in detail elsewhere.[15,18] The method involves fitting the experimental absorption data to the theoretical standards calculated from FEFF.[30] The fitting of the FEFF theoretical standards to the experimental data was accomplished using an analysis program (FEFFIT)[31] that employs a nonlinear, least-squares technique.

III. RESULTS AND DISCUSSION

Figure 2 presents two x-ray transmission images. Image A is from the microreactor cell at 100 °C that was initially loaded with CuO and Cu^0 solids and an aqueous solution of 0.5 m NaCl at a *p*H of 0.5. Image B is from the microreactor cell at 325 °C initially loaded with Cu^0 and an aqueous solution of 0.2 m $CuCl_2$ at a *p*H of 1.5. For the system at 100 °C in Fig. 2(A), four different phases coexist. These include the added CuO that can be observed along the lower perimeter of the cell in the image of Fig. 2(A). In addition, there is a liquid phase with soluble Cu(I) species in equilibrium with the vapor phase (large circular bubble at the top of the cell). Finally there is the Cu^0 phase of the internal surface of the cell walls. For the solution in Fig. 2(A), the aqueous phase that is initially loaded into the cell contained 0.5 m NaCl at *p*H 0.5. For the solution in Fig. 2(B) that is at

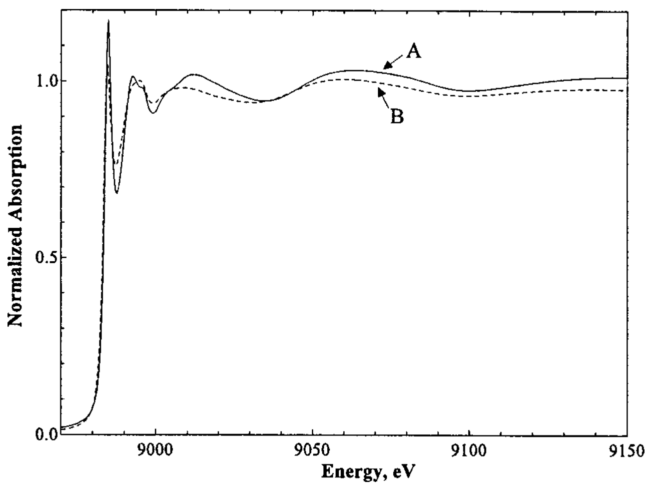

FIG. 3. X-ray absorption spectra at the Cu K-edge for two solutions corresponding to locations marked in the images in Fig. 2 and the starting compositions reported in Table I. The two spectra were scaled to a common edge height.

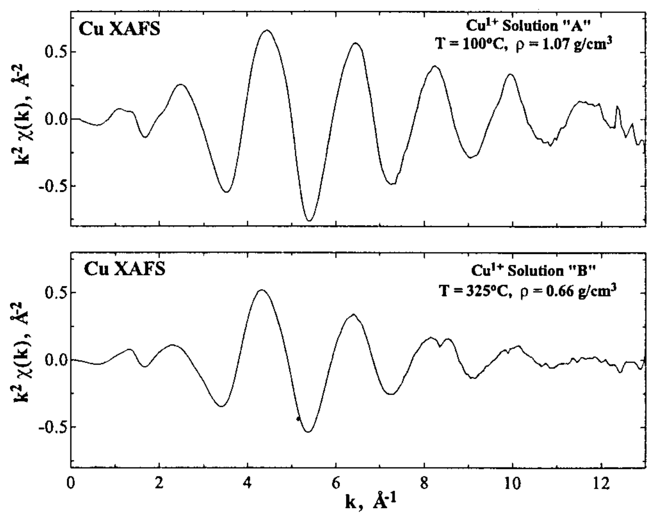

FIG. 4. Cu EXAFS k^2-weighted $\chi(k)$ plots for two Cu^{1+} solutions whose starting compositions are reported in Table I.

325 °C, a three-phase mixture exists in which the Cu^0 of the cell walls is in equilibrium with a liquid and a vapor phase. In this case, the starting solution initially contains 0.2 m $CuCl_2$ at a pH of 1.5. In the images of Fig. 2, the spatial isolation of the various phases is sufficient to acquire micro-XAFS in each region without interference from the other phases.

The copper redox chemistry occurring in the solutions of Figs. 2(A) and 2(B) can be summarized in the following way:

$$CuO+Cu^0+4Cl^-+2H^+ \underset{T>100\,°C}{\rightarrow} 2[CuCl_2]^-+H_2O, \quad (1)$$

$$[Cu(H_2O)_6]^{2+}+Cu^0+4Cl^- \underset{T>100\,°C}{\rightarrow} 2[CuCl_2]^- +6H_2O. \quad (2)$$

In both cases the starting Cu(II) species are reduced to Cu(I) by the Cu^0 of the cell tube. Because the wetted internal surfaces of the cell contain only pure copper metal and diamond there is no possibility of other contaminating metals interfering with this redox chemistry. In other studies we have found that Cu^{2+} readily oxidized noble metals like Pt and Ir in high-temperature aqueous solutions, epecially in the presence of complexing halide ions.[25] The chemical strategy outlined in Eqs. (1) and (2) allows one to quantitatively prepare a Cu^{1+} for high temperature studies with no possibility of contamination from other metals.

Figure 3 shows the x-ray absorption spectra for each of the solutions in Fig. 2. The spectra were acquired at positions within the cell that contained only the liquid phase (see Fig. 2). One of the dominant features of these near-edge spectra is the narrow and strong absorption band at about 8984 eV that is assigned to the $1s\rightarrow4p$ bound-state transition. One can readily observe the dramatic transition in the pre-edge structure upon heating the Cu^{2+} solution to Cu^{1+} in the high-pressure XAFS cell where the reactions according to Eqs. (1) and (2) occur. For the hexaaqua Cu^{2+} species, the $1s\rightarrow4p$ transition is formally forbidden. Quantitative analysis of this pre-edge peak height shows that for solution A (see Table I) the dissolved copper is fully in the Cu(I) state. For solution B, the slightly reduced amplitude means that there is still about 10% Cu(II) in addition to the Cu(I) in solution.

In Fig. 3, the oscillations in the spectra above 9000 eV are primarily due to photoelectron backscattering from the Cl^- in the first coordination shell about the Cu^{1+}. Figure 4 shows these oscillations in the Cu K-edge EXAFS spectra (k^2-weighted $\chi(k)$ data) that have been extracted from the spectra of Fig. 3 by removal of the Cu background function. Figure 5 gives the $\tilde{\chi}(R)$ results that represent the magnitude of the Fourier transformed $\chi(k)$ data given in Fig. 4. The $\tilde{\chi}(R)$ functions are closely related to the standard radial, partial-pair distribution functions with the difference that for distances greater than about 4 Å the $\tilde{\chi}(R)$ results are strongly damped by the convolution with the photoelectron scattering functions and by the large structural disorder of the atoms beyond the first shell. The backscattering amplitude of O from the first-shell hydration water is very strong in the re-

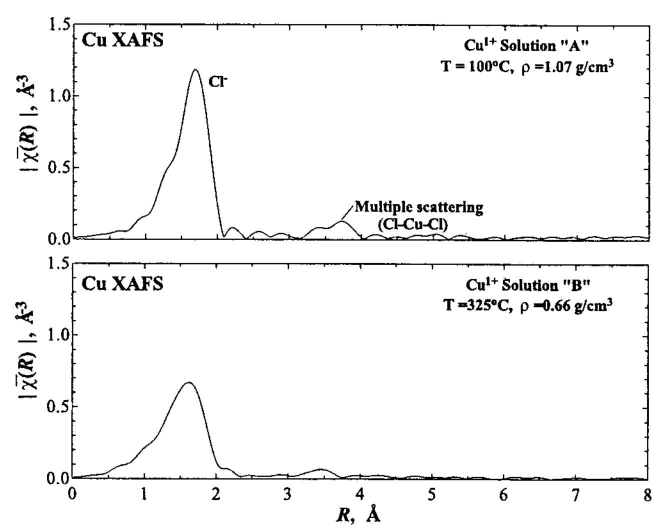

FIG. 5. The $|\tilde{\chi}(R)|$ plots from the magnitude of the Fourier transform of the $\chi(k)$ spectra shown in Fig. 4. This $|\tilde{\chi}(R)|$ plot is uncorrected for phase shifts whereas the actual distances are reported in Table II.

TABLE II. Cu(I,II) speciations under hydrothermal conditions for solutions corresponding to those in Figs. 2(A) and 2(B) after reduction of the Cu(II) starting compounds. The starting compositions under ambient conditions are reported in Table I. Results of Cu XAFS analysis of first-shell Cu(I,II) structures. Concentrations are expressed in molality. Uncertainties are given in parentheses.

System			Conditions		Structure			
Solution	Components	Scatterer	T (°C)	ρ (g/cm^3)	N	R (Å)	$\sigma^2 \times 10^3$ (Å^2)	$\mathfrak{R}^a$
A	0.3 m $Cu^{I}Cl_2^-$	Chlorine	100	1.07	1.9(0.1)[b]	2.14(0.01)	4.8(0.5)	0.013
	0.3 m HCl/0.5 m NaCl							
B	0.2 m $Cu^{I}Cl_n^{1-n}(H_2O)_m$	Chlorine	325	0.66	1.6(0.6)[b]	2.11(0.03)	23(10.2)	0.017
	$Cu^{II}Cl_n^{2-n}(H_2O)_m$	Oxygen			0.7(0.4)	2.01(0.08)	6.6(8.2)	
	0.03 m HCl							

[a]Goodness of fit defined by a scaled sum of squares as described in FEFFIT (Ref. 31).
[b]Fit includes multiple scattering paths for linear Cl atoms.

gion from 8990 to about 9050 eV, and these features are lacking in the Cu^{1+} spectra of Fig. 4. Upon heating ambient solutions that contain the hexaaqua Cu^{2+} species to higher temperatures where complete conversion to Cu^{1+} occurs, a strong and broad Cu–O band at 9000 eV mostly disappears. This is qualitative evidence that the new $CuCl_2^-$ species is not strongly hydrated with water in the first shell. This aspect is reinforced by the results reported in Table II for the quantitative fits of the data to the theoretical standards.[30,31] Significantly, the coordination structure for the Cu^{1+} ion (solution A) contains only 2 Cl^- at a distance of about 2.14 Å. The coordination structure observed for this copper chloride system is nearly identical to the chemistry and structure that have recently been extensively examined in detail for the copper bromide system.[25] A more detailed treatment of this Cu–Cl coordination is given elsewhere.[32]

For solution B the structural picture is slightly different because the Cl^- and hydrogen ion concentrations are too low to obtain complete conversion to $CuCl_2^-$. In this case, the analysis of the pre-edge peak height indicates that about 10% Cu(II) remains in solution. Quantitative analysis of the XAFS spectra reported in Table II indicates that the Cu is still predominantly coordinated with the Cl^- but in this case, there is still some significant amount of O in the first shell from either H_2O, or possibly from OH^-.

It is important to realize that the results presented here may not necessarily represent the equilibrium concentrations. This can be verified by testing the reversibility of the equilibrium at high temperature. It is also unrealistic to expect that the technique will be used to explore *equilibrium* conditions at temperatures much below 200 °C since the kinetics for many systems are prohibitively long under these circumstances. The Cu system of this study seems to be an exception because it is already highly reactive at slightly elevated temperatures. This technique could also yield kinetic information if temperatures were selected such that the rates of reaction could be tracked using prominent pre-edge features of some of the transition metals.

For the systems under investigation here there are only one or two predominant species that are in solution under hydrothermal conditions. For system in which multiple species are dissolved, the analysis of the XAFS data becomes more difficult. Clearly, deconvoluting strong pre-edge peaks can yield the relative percentages of various oxidation states. In these cases, the analysis of the coordination structure from the EXAFS region for the individual species is more problematic. One strategy is to use FEFF in conjunction with a thermodynamic model. The speciation is predicted from the models which can be used as input into the FEFF program that provides theoretically derived XAFS spectra that can then be directly compared to the experiment. A related strategy has already been used successfully to test coordination structure and intermolecular potentials from molecular dynamics simulations.[10,15,17]

ACKNOWLEDGMENTS

This research was supported by the Director, Office of Energy Research, Office of Basic Energy Sciences, Chemical Sciences Division of the U.S. Department of Energy, under Contract No. DE-AC06-76RLO 1830. Work by two of the authors (J.G.D. and M.M.H.) was supported by the U.S. Department of Energy, Office of Environmental Management, under Contract No. DE-AC06-76RLO 1830. Pacific Northwest National Laboratory is operated by Battelle Memorial Institute.

[1] D. W. Matson, J. C. Linehan, J. G. Darab, M. F. Beecher, M. R. Phelps, and G. G. Neuenschwander, in *Advanced Catalysts and Nanostructured Materials*, edited by W. R. Moser (Academic, San Diego, CA, 1996), pp. 259–283.
[2] J. G. Darab and D. W. Matson, J. Electron. Mater. **27**, 1068 (1998).
[3] M. H. Langowski, J. G. Darab, and P. A. Smith, Westinghouse Hanford Company letter report, Richland, WA 99352, 1995, PVTD-C-95-02.03G.
[4] J. G. Darab and P. A. Smith, Chem. Phys. **8**, 1004 (1996).
[5] H. L. Barnes and A. W. Rose, Science **279**, 2064 (1998).
[6] T. B. Brill and P. D. Spohn, J. Phys. Chem. **93**, 6224 (1989).
[7] B. Scholz, H. D. Lüdemann, and E. U. Franck, Ber. Bunsenges. Phys. Chem. **76**, 413 (1972).
[8] C. A. Angell and D. M. Gruen, J. Am. Chem. Soc. **88**, 5192 (1966).
[9] D. M. Pfund, J. G. Darab, J. L. Fulton, and Y. Ma, J. Phys. Chem. **98**, 13102 (1994).
[10] B. J. Palmer, D. M. Pfund, and J. L. Fulton, J. Phys. Chem. **100**, 13393 (1996).
[11] J. L. Fulton, D. M. Pfund, S. L. Wallen, M. Newville, E. A. Stern, and Y. Ma, J. Chem. Phys. **105**, 2161 (1996).
[12] S. L. Wallen, B. J. Palmer, and J. L. Fulton, J. Chem. Phys. **108**, 4039 (1998).
[13] T. M. Seward, C. M. B. Henderson, J. M. Charnock, and B. R. Dobson, Geochim. Cosmochim. Acta **60**, 2273 (1996).
[14] K. V. Ragnarsdottir, E. H. Oelkers, D. M. Sherman, and C. R. Collins, Chem. Geol. **151**, 29 (1998).
[15] M. M. Hoffmann, J. G. Darab, B. J. Palmer, and J. L. Fulton, J. Phys. Chem. A **103**, 8471 (1999).

[16] T. M. Seward, C. M. B. Henderson, J. M. Charnock, and T. Driesner, Geochim. Cosmochim. Acta **63**, 2409 (1999).
[17] S. L. Wallen, B. J. Palmer, D. M. Pfund, J. L. Fulton, M. Newville, Y. Ma, and E. A. Stern, J. Phys. Chem. A **101**, 9632 (1997).
[18] M. M. Hoffmann, J. G. Darab, S. M. Heald, C. R. Yonker, and J. L. Fulton, Chem. Geol. **167**, 89 (2000).
[19] J. L. Fulton, D. M. Pfund, and Y. Ma, Rev. Sci. Instrum. **67**, 1 (1996).
[20] J. F. W. Mosselmans, P. F. Schofield, J. M. Charnock, C. D. Garner, R. A. D. Pattrick, and D. J. Vaughan, Chem. Geol. **127**, 339 (1996).
[21] W. A. Bassett, A. J. Anderson, R. A. Mayanovic, and I. M. Chou, Chem. Geol. **167**, 3 (2000).
[22] T. Murata, K. Nakagawa, A. Kimura, N. Otoda, and I. Shimoyama, Rev. Sci. Instrum. **66**, 1437 (1995).
[23] Z. Xiao, C. H. Gammons, and A. E. Williams-Jones, Geochim. Cosmochim. Acta **62**, 2949 (1998).
[24] B. W. Mountain and T. M. Seward, Geochim. Cosmochim. Acta **63**, 11 (1999).
[25] J. L. Fulton, M. M. Hoffmann, J. G. Darab, B. J. Palmer, and E. A. Stern, J. Phys. Chem. A **104**, 11651 (2000).
[26] R. Ingalls, E. D. Crozier, J. E. Whitmore, A. J. Seary, and J. M. Tranquada, J. Appl. Phys. **51**, 3158 (1986).
[27] B. K. Teo, EXAFS: *Basic Principles and Data Analysis* (Springer, New York, 1986).
[28] E. A. Stern and S. Heald, in *Handbook of Synchrotron Radiation*, edited by D. E. Farge and E. E. Koch (North-Holland, Amsterdam, 1983).
[29] *X-Ray Absorption: Principles, Applications, Techniques of EXAFS, SEXAFS, and XANES*, edited by D. C. Koningsberger and R. Prins (Wiley, New York, 1988).
[30] S. I. Zabinsky, J. J. Rehr, A. Ankudinov, R. C. Albers, and M. J. Eller, Phys. Rev. B **52**, 2995 (1995).
[31] M. Newville, R. Ravel, D. Haskel, J. J. Rehr, E. A. Stern, and Y. Yacoby, Physica B **208&209**, 154 (1995).
[32] J. L. Fulton, M. M. Hoffmann, and J. G. Darab, Chem. Phys. Lett. **330**, 300 (2000).